

# A Pinchable Aerial Virtual Sphere by Acoustic Ultrasound Stationary Wave

Seki Inoue\*

Hiroyuki Shinoda†

Graduate School of Information Science and Technology, The University of Tokyo‡

## ABSTRACT

In this paper, we propose a system to generate aerial virtual spheres which invokes tactile sensation and is omni-directionally pinchable. The acoustic radiation force of ultrasound stationary waves is known in the field of non-contact micro manipulation. This force applied to a small object in the stationary wave is in proportion to the gradient of the square of the acoustic pressure and directing from anti-node to node. We demonstrate a prototype system consisting of 996 transducers which generates a focal anti-node point at the center of the workspace. We performed the acoustic pressure distribution analysis and subjective experiments. As a result, it is discovered that the virtual sphere was sensed as the same size as theoretically expected.

**Keywords:** Aerial tangible virtual objects, Acoustic radiation pressure, Tactile feedback, Airborne ultrasound tactile display.

**Index Terms:** H.5.2 [Information Interfaces and Presentation]: User Interfaces—Haptic I/O; I.3.7 [Computer Graphics]: Three-Dimensional Graphics and Realism—Virtual reality

## 1 INTRODUCTION

The presentation of tactile sensation for virtual 3D objects have been in great interest. The addition of a tactile property to aerial 3D images may bring truly realistic virtual perception to us. To this end, we still have a long journey and we think there are three major issues to be solved. First, the haptic device should not affect optical pictures. Second, the haptic device should not hinder user's action. Third, the position or shape of presented haptic objects should be flexible.

For years, mechanical approaches have been researched for 3D haptic presentation. For example, using pen-type pointing devices like PHANTOM™ or glove-type master-slave systems[1] have succeeded to present relatively strong and accurate force feedback. However, in this strategy, the skin and the device are always in contact and leading to prevent free motion. Recent vibrotactile approaches have made the devices simplified and wearable, but users still have to touch the virtual objects via special devices[2]. Another approach is also proposed to present tactile sensation at a distance without any direct contact. For example, using air-jets enables to realize non-contact force feedback[3]. However, its spatial and temporal profiles are quite rough.

We have proposed a method for producing tactile sensation using airborne ultrasound[4]. Especially in [5], a system which adds a tactile feedback to hologram image was proposed. The airborne ultrasound tactile display (AUTD) utilizes the acoustic radiation pressure so that users can feel the force with their bare hands. The ultrasound emitters of the AUTD serve as a phased array allowing the steering of a focal point i.e. sense point. However, there are some

problems in this system. First, the focal point is somewhat spatially spread and therefore the possible spatial patterns is limited. One solution is increasing the frequency and shortening the ultrasound wavelength. But the problem is that a high frequency ultrasounds strongly attenuates in the mid-air. Second, it is also pointed out that air flow around the focal point which deteriorate the tactile sensation is generated. Third, these systems radiate one-way progressive wave and therefore limiting the tactile sensation one-direction.

In this paper, we propose a method to invoke more vivid and omni-directional haptic sensation using airborne ultrasounds. By placing ultrasound transducers face to face, stationary waves arise and that create 1) smaller focal points, 2) negligible air flow and 3) virtual omni-directionally compliant objects. As a result, a truly pinchable virtual sphere is generated. The system and its analysis and experiments are described.

## 2 SYSTEM OVERVIEW

### 2.1 Principle

Many studies have investigated the acoustic radiation pressure for stationary waves mainly in the field of non-contact micro manipulation[6][7].

The acoustic radiation force on a small rigid spherical object in the stationary plane wave field is expressed as below[8]:

$$F = VD\nabla\overline{K_E} - V(1-\gamma)\nabla\overline{P_E} \quad (1)$$

$$D = \frac{3(\rho - \rho_0)}{2\rho + \rho_0} \quad (2)$$

where  $V$  is the volume of the spherical object,  $\rho$  is the density of the object,  $\rho_0$  is the density of the air and  $\gamma$  is the ratio of the compressibility of the air to that of the spherical object.

$\overline{K_E}$  and  $\overline{P_E}$  are time averaged kinetic and potential energy respectively. They are described as follows:

$$\overline{K_E} = \frac{1}{2}\rho_0\overline{v^2}, \quad \overline{P_E} = \frac{1}{2\rho_0c^2}\overline{p^2}, \quad (3)$$

where  $c$  is the speed of sound in air,  $v$  is the particle velocity and  $p$  is the acoustic pressure.

Under the stationary plane wave circumstance, following can be assumed.

$$\nabla\overline{K_E} + \nabla\overline{P_E} \sim 0 \quad (4)$$

So, the acoustic radiation force is written as

$$F = -\frac{V}{2\rho_0c^2} \left( \frac{5\rho - 2\rho_0}{2\rho + \rho_0} - \gamma \right) \nabla\overline{p^2} \quad (5)$$

This shows that the force applied to a small object in the acoustic field is in proportion to the gradient of the square of time-averaged pressure in the field. Hence  $\rho \gg \rho_0$ , the force directs from anti-nodes to nodes. It should be noted that this result is valid under the stationary plane wave field and more precise discussion will be needed.

\*E-mail: seki.inoue@ipc.i.u-tokyo.ac.jp

†E-mail: hiroyuki.shinoda@k.u-tokyo.ac.jp

‡Address: Room 622, Engineering Building #14, Hongo Campus, The University of Tokyo 7-3-1, Hongo, Bunkyo-ku, Tokyo, Japan

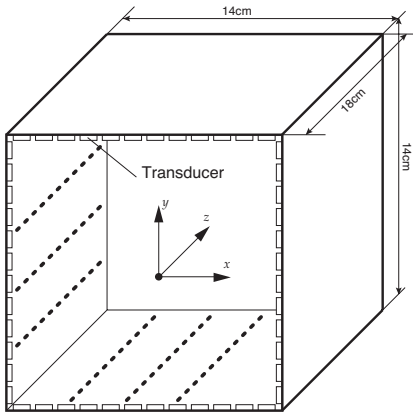


Figure 1: System overview. Transducers are arranged face to face and it generates a focal point.

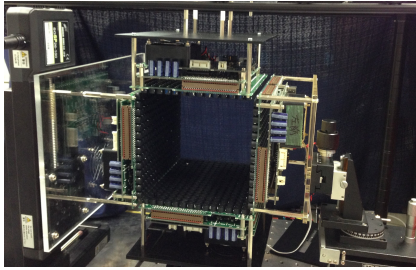


Figure 2: An overall picture of the system. 4 arrays with 249 transducers, a total of 996 transducers are arranged that forms rectangular parallelepiped.

## 2.2 Prototype System

We built a prototype system as shown in figure 1 and figure 2. In this system, transducers are arranged to surround a user workspace. A single unit of transducer array consists of 249 transducers and has  $14\text{ cm} \times 18\text{ cm}$  area. 4 units form a rectangular parallelepiped workspace. So the workspace became  $14\text{ cm} \times 14\text{ cm} \times 18\text{ cm}$ .

Each transducer emits 40 kHz ultrasound and their amplitude and phase are electronically controlled. In this study, in order to generate a single focal point, a transducer at a position  $r = (x, y, z)$  emits a signal as follows:

$$p(r, t) = A \sin \left( 2\pi f \left( t + \frac{|r - r_f|}{c} \right) \right) \quad (6)$$

where,  $r_f$  is the focal point,  $f = 40\text{ kHz}$  is the frequency, and  $c = 340.31\text{ m/s}$  is the sound speed. In this paper the focal point is fixed to the center of the workspace, where the center is defined as the origin, namely  $r_f = (0, 0, 0)$ .

## 2.3 Virtual Sphere

The prototype system described above generates the ultrasound pressure distribution. Putting fingers into the workspace, the aerial spherical object is sensed. The aerial object is pinchable and compliant. It should be noticed that Equation (5) is valid only when a sphere is sufficiently small that does not affect the acoustic field. It is our future work to quantitatively evaluate the effect of occlusion and interference by user's fingers and palm. At least in our experiment, however, the effect was negligible and the sphere could be

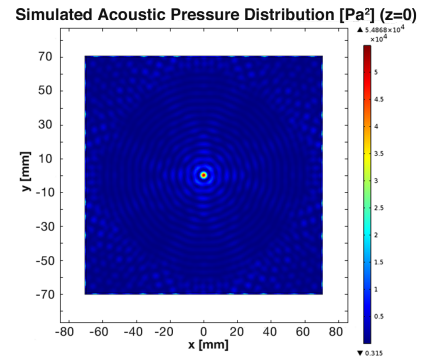


Figure 3: Simulated acoustic distribution on a plane  $z = 0$ . A focal point at origin appears.

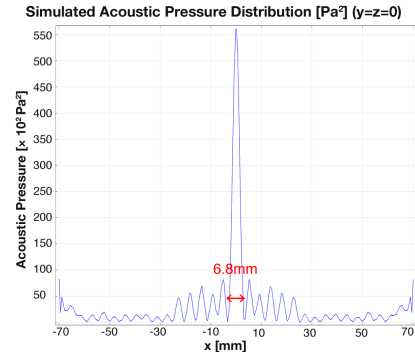


Figure 4: Simulated acoustic distribution on a line  $y = z = 0$

roughly grasped. It is noteworthy that the absence of air flow makes the haptic image clearly.

## 3 SIMULATION

To visualize the acoustic field of the working space, numerical simulation by Finite Element Method was conducted. We used COMSOL Multiphysics 4.3b and the size and the number of transducers were arranged as actual scale. For simplicity, all boundaries including transducers and the two openings facing in  $z$ -axis were set to have perfectly matched impedance. This simplification is valid because the transducer's impedance are matched with air and therefore quit few reflection will occur.

The results are shown in figure 3 and figure 4. On the space  $z = 0$ , an circular pattern appears and a clear focal point is emerged. On the line  $y = z = 0$ , the full width at half maximum of the focal point is 5.6 mm and the distance of the primal nodes is 6.8 mm.

For comparison, a situation where only there is only one unit is also simulated. This generates a conventional one-way progressive wave. Figure 5 and figure 6 show the results. In this case, the distance of the primal nodes is 10.2 mm. It is obvious that focal point became significantly smaller and therefore it is expected that invoked sensation became stronger if equal energy was transmitted in the focal point.

## 4 EXPERIMENTS

### 4.1 Pressure Distribution

To confirm the result of numerical simulation, the actual acoustic pressure distribution was measured. As shown in figure 7, the microphone with diameter of 1/4 inch was pointed in parallel with the

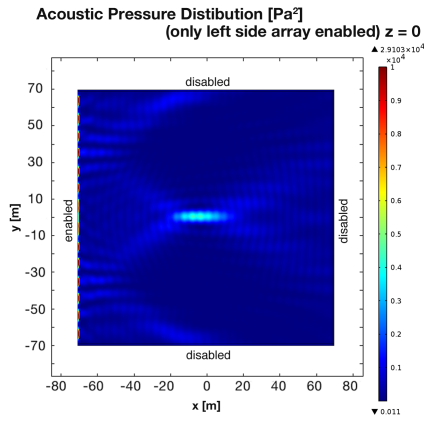


Figure 5: Simulated acoustic distribution on a plane  $z = 0$ . Only the left phased array is activated. A focal point at origin appears but it widens largely towards the progress direction.

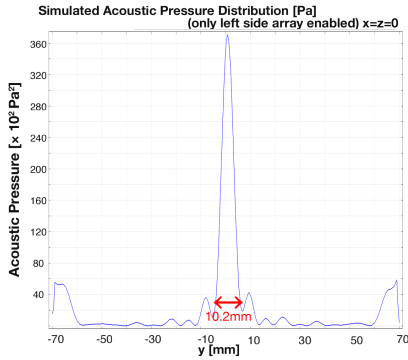


Figure 6: Simulated acoustic distribution on a line  $x = z = 0$ . Only the left phased array is activated.

phased arrays. Utilizing motorized 3-axis stage, the acoustic pressure was measured around a focal point by 0.25 mm intervals.

The result is described in figure 8 - 10. Figure 8 and 9 show the 2D distribution of the squared acoustic pressure. Towards  $x$  and  $y$  axes - transducers exist - the pressure distributes isotropically and forms a circle. In contrast, an elliptic distribution appears towards  $z$  axis because there are no transducers in this direction.

Figure 10 shows the distribution on the line of  $y = z = 0$ . The interval between node to node is 7.5 mm. This diameter is 1.11 times larger than that of simulation in figure 4. The sidelobes are slightly spread but the shape is quite resemble.

## 4.2 Subjective Experiment

To investigate how the virtual sphere is realized by users, we conducted tests to ask the perceived sphere diameter. We prepared nine nylon balls with various diameters. The sizes are shown in Table 1. Examinees were handed a ball and requested to compare and answer which is bigger or equal. It was forbidden for examinees to see the nylon balls directly and requested to judge only by the sense of touch. There was no time restriction to answer. The question is repeated with different ball sizes. The operations are conducted in according with staircase method. A scene of this experiment is described in figure 11. During this experiment, the pressure of the center of the sphere were 221.5 Pa. All the examinees were males in twenties. The first author was one of the examinees as number 3.



Figure 7: The scene of experiments to measure the actual pressure distribution. The microphone whose diameter is 1/4 inch are mounted on 3-axis motorized stage and was pointed in parallel with phased array.

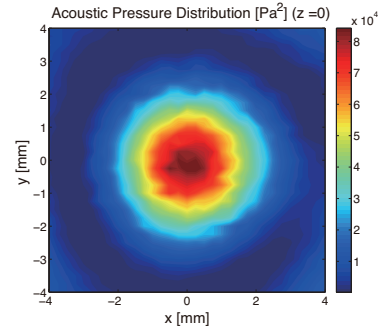


Figure 8: Measured acoustic distribution on a plane  $z = 0$ . A spherical focal point at origin appears.

The result by 9 examinees is shown in figure 12. Values for each examinees is a mean of diameters which is perceived identical to virtual sphere. The error bar shows the maximum and minimum diameters.

The mean across examinees is 7.92 mm and its standard deviation is 1.23 mm. According to the simulation result, the diameter actually sensed is slightly larger but roughly equal to that of the node plane of actual pressure distribution.

## 5 CONCLUSION

In this paper, we proposed a system to produce a pinchable aerial virtual sphere by using acoustic ultrasound stationary wave. We arranged 996 transducers face to face each other and shifted the phase of signal outputted from them, smaller focal point was created compared with the previous work. This focal point has a spherical shape and acoustic radiation pressure invoked is isotropic. This is confirmed by numerical simulation and measurement. Besides, a test to determine how people perceive the aerial virtual sphere is conducted. With staircase method inquiry, it is discovered that the sphere size is sensed almost as the same as that of the focal point. This sphere is pinchable from any direction and has spatial expanse. The possible applications are such as the combination with 3D images and finger location detectors.

The further works are as follows: 1) To investigate the strength of force on fingers. It is also interesting to see how the force intensity varies with size, position and form of fingers. 2) To optimize the frequency of the ultrasound. According to Equation (5), it is seen that the force is in proportion to the frequency. On the other hand, the higher frequency causes the more rapid attenuation. So, there should be the optimum value. 3) To establish the control method to create arbitrary spatial form such as larger spheres or cubes.

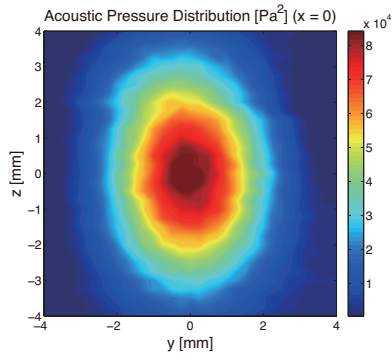


Figure 9: Measured acoustic distribution on a plane  $x = 0$ . An elliptic focal point at origin appears.

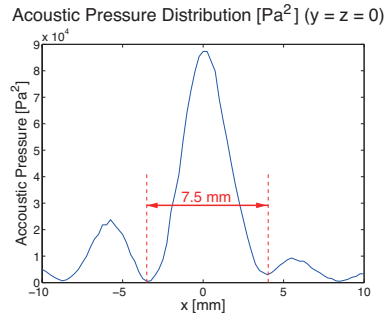


Figure 10: Measured acoustic distribution on a plane  $y = z = 0$ . A focal point appears and its diameter is 7.5 mm.

|   | (inch) | (mm)  |
|---|--------|-------|
| 1 | 3/32   | 2.38  |
| 2 | 1/8    | 3.175 |
| 3 | 5/32   | 3.96  |
| 4 | 3/16   | 4.75  |
| 5 | 7/32   | 5.56  |
| 6 | 1/4    | 6.35  |
| 7 | 5/16   | 7.94  |
| 8 | 3/8    | 9.53  |
| 9 | 1/2    | 12.7  |

Table 1: The size list of nylon balls used as reference.

## REFERENCES

- [1] D. Jack, R. Boian, A.S. Merians, M. Tremaine, G.C. Burdea, S.V. Adamovich, M. Recce, and H. Poizner. Virtual reality-enhanced stroke rehabilitation. *Neural Systems and Rehabilitation Engineering, IEEE Transactions on*, Vol. 9, No. 3, pp. 308–318, 2001.
- [2] Kouta Minamizawa, Yasuaki Kakehi, Masashi Nakatani, Soichiro Mihara, and Susumu Tachi. Techtile toolkit: a prototyping tool for designing haptic media. In *ACM SIGGRAPH 2012 Emerging Technologies, SIGGRAPH '12*, pp. 22:1–22:1, New York, NY, USA, 2012. ACM.
- [3] Y. Suzuki and M. Kobayashi. Air jet driven force feedback in virtual reality. *Computer Graphics and Applications, IEEE*, Vol. 25, No. 1, pp. 44–47, 2005.
- [4] T. Hoshi, M. Takahashi, T. Iwamoto, and H. Shinoda. Noncontact tactile display based on radiation pressure of airborne ultrasound. *Haptics, IEEE Transactions on*, Vol. 3, No. 3, pp. 155–165, 2010.
- [5] T. Hoshi, D. Abe, and H. Shinoda. Adding tactile reaction to hologram. In *Robot and Human Interactive Communication, 2009. RO-MAN 2009. The 18th IEEE International Symposium on*, pp. 7–11, 2009.
- [6] R. R. WHYMARK. Acoustic field positioning for containless processing. *Ultrasonics*, Vol. 13, pp. 251–261, 1975.
- [7] D. Koyama and K. Nakamura. Noncontact ultrasonic transportation of small objects over long distances in air using a bending vibrator and a reflector. *Ultrasonics, Ferroelectrics and Frequency Control, IEEE Transactions on*, Vol. 57, No. 5, pp. 1152–1159, 2010.
- [8] W. L. Nyborg. “Physical principles of ultrasound,” in *Ultrasound: Its Applications in Medicine and Biology* Amsterdam. The Netherlands: Elsevier scientific Publishing company, 1978.

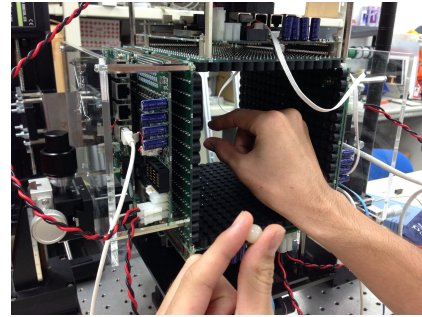


Figure 11: A scene of subjective sensation experiment. Under blind circumstance, examinees were handed a ball and request to answer which is bigger or equal.

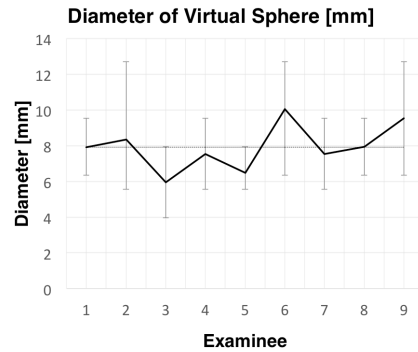


Figure 12: The result of subjective sensation experiment. Values for each examinee is mean of diameters which is sensed identical to virtual sphere. The error bar shows the maximum and minimum diameter which is sensed identical to virtual sphere. The mean across examinees is 7.92 mm and its standard deviation is 1.23 mm.